Rapid magnitude determination for earthquake early warning

Richard M Allen – University of Wisconsin-Madison
Email: rallen@geology.wisc.edu Tel: +1 608 262 7513 Fax: +1 608 262 0693

in "The Many Facets of Seismic Risk" edited by G. Manfredi, M.R. Pecce, and A. Zollo, Universita degli Studi di Napoli "Federico II", Napoli, Italy, p15-24, 2004.
This is the proceedings of the "Workshop on Multidisciplinary Approach to Seismic Risk Problems," Sant'Angelo dei Lombardi, September 22, 2003.

Introduction

The goal of an earthquake early warning system is to provide notification of ground shaking hazard before significant ground motion is felt. An operational system requires four components: (1) seismic network infrastructure, (2) rapid event characterization, (3) spatial hazard prediction, and (4) a notification system to warn of hazard. Here I present an overview of such an early warning system designed for use with a dense seismic network in the earthquake source region. Emphasis is placed on components (2) and (3) as they are common to implementation of the system in any region. The particular example described is for southern California; however, the same methodology could be utilized in the Irpinia region of Italy.

In many earthquake prone regions, including California, Japan, Taiwan, Italy, and Turkey, population centers are collocated with the earthquake source region. In such a case, hazard must be determined using the low amplitude P-wave which can be detected seconds before significant ground motion begins. The earthquake early warning methodology described here, named ElarmS, uses the P-wave arrival to estimate hazard and therefore has the potential to issue warning before damaging ground shaking begins, even at the epicenter of an earthquake.

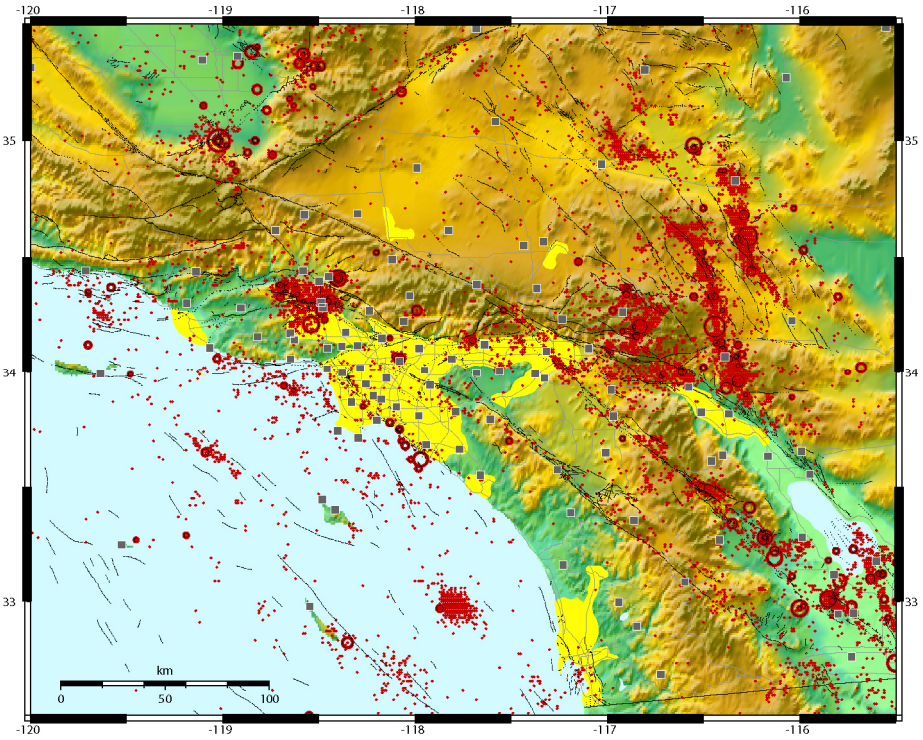

Fig. 1. Map of southern California showing the collocation of known faults (black lines), past earthquake epicenters (red dots for magnitude < 5 and black circles for mag > 5) and population centers (bright yellow). The seismic stations belonging to TriNet and capable of onsite data processing are shown as grey squares. Station density is greatest in at-risk populated areas where the typical station spacing is ~25 km.

1. Seismic network infrastructure

The network infrastructure required consists of seismometers and a rapid telemetry system. Fig. 1 shows the seismic network in southern California, TriNet [*Kanamori et al.*, 1997; *Hauksson et al.*, 2001]. Station density is greatest where population (yellow regions, Fig. 1) coincides with earthquake source regions represented by known faults (black lines) and earthquake epicenters (red dots). In these regions the typical stations spacing is ~25 km. Such dense coverage is important as the accuracy of the magnitude estimate increases with the number of stations recording the P-wave arrival. Rapid telemetry is also central to an effective warning system, since any delay in transmittal of information from seismic station to the central processing site is a delay in the issuance of a warning. Communication delay can be minimized by processing waveforms at the seismic stations and transmitting only parameter information to the central processing site.

2. Event characterization: magnitude

To predict the hazard posed by an earthquake two event parameters are needed: location and magnitude. Earthquake location can be determined using a similar approach to normal network operation based on P-wave arrival times. Initially, an event is located at the site of the first station to trigger, then between the first two, and then first three stations. Once arrival times at four stations are known, the event can be accurately located using normal techniques. Local earthquake magnitude is usually determined using peak ground motion observations, i.e. it is not available in time to issue a warning. An alternative approach to magnitude determination must therefore be developed using the P-wave arrival.

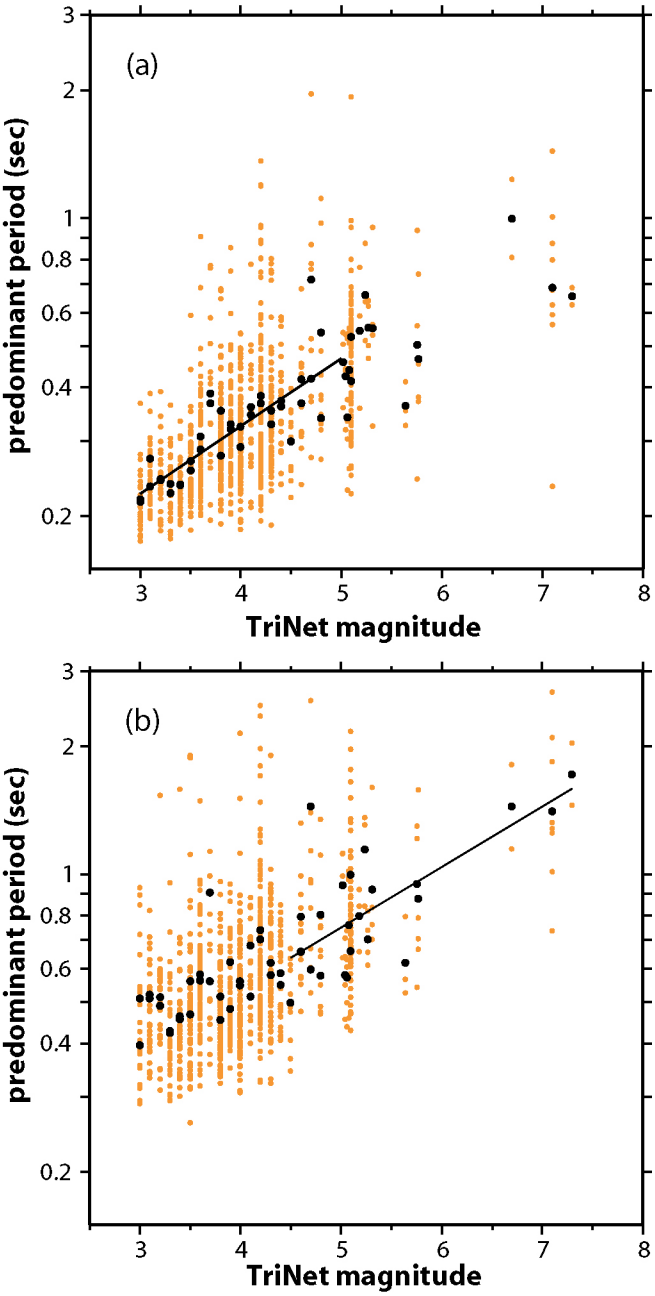

Fig. 2. Relation between predominant period and magnitude. Predominant period measured on the vertical component of a broadband velocity sensor. (a) Maximum predominant period observed within 2 seconds of the P-wave arrival low-pass filtered at 10 Hz versus TriNet magnitude for individual stations (gray dots) and event averages (black dots) for all 53 events. The black line is the best fit (least absolute deviation of event averages) for data from magnitude 3.0 to 5.0 events. (b) as (a) except maximum predominant period within 4 seconds of the P-arrival on the same data stream low-pass filtered at 3 Hz. The black line is the best fit to event averages for earthquakes with magnitude between 5.0 and 7.3. Observations of predominant period at single stations show significant scatter (gray dots), but once several stations are averaged the scatter is reduced significantly (black dots).

ElarmS rapidly determines magnitude based on the frequency content of the P-wave. Small earthquakes rupture small fault patches generating a high frequency signal, while large events rupture large faults generating a lower frequency signal. The frequency content is characterized using the predominant period, T^p, which is determined in realtime from the vertical component of a velocity sensor [*Nakamura*, 1988; *Allen and Kanamori*, 2003]. Fig. 2 shows the relationship between the T^p and magnitude determined using 53 earthquakes in southern California ranging in magnitude from 3.0 to 7.3. The relation for low-magnitude events (mag < 5, Fig. 2a) is determined using the maximum predominant period, $T^p_{\max}$, within 2 seconds of the P-wave trigger having low-passed the data at 10 Hz. For larger magnitude events (Fig. 2b) better magnitude estimates require 4 seconds of data and a low-pass filter of 3 Hz. Earthquake magnitude can therefore be determined using the following relations:

$$m_l = 6.3\log\left(T^p_{\max}\right) + 7.1; \quad m_h = 7.0\log\left(T^p_{\max}\right) + 5.9$$

where m_l and m_h are the magnitude estimates for low-magnitude and high-magnitude events respectively [*Allen and Kanamori*, 2003]. Waveform datasets from other regions including the Pacific Northwest of the U.S. and Japan show similar magnitude period relations [*Lockman and Allen*, in preparation].

ElarmS uses a realtime approach to magnitude determination. Fig. 3 shows the progression of the magnitude determination using the predominant frequency ($f^p = 1/T^p$) trace calculated from the vertical velocity recorded at a station 50 km from the epicenter of a magnitude 3.9 earthquake. After the P-wave trigger, the first 0.5 sec of f^p is ignored as it contains transients between the frequency content of background noise and the P-wave arrival. The first magnitude estimate is available 1 sec after the trigger. It is calculated from the minimum f^p between 0.5 and 1 sec using the magnitude-period relation shown in Fig. 2a. In the example shown in Fig. 3 the minimum f^p is 3.10 Hz providing a magnitude estimate of 4.0. ElarmS then continues to monitor f^p for the 2nd second. If f^p should drop lower than what was observed during the 1st second, it would represent a new $T^p_{\max}$ and would be used to generate a new magnitude estimate that would be greater than the initial estimate. This does not occur in the example shown in Fig. 3; the best magnitude estimate in this case is available within 1 sec of the P-wave arrival and has an error of 0.1 magnitude units.

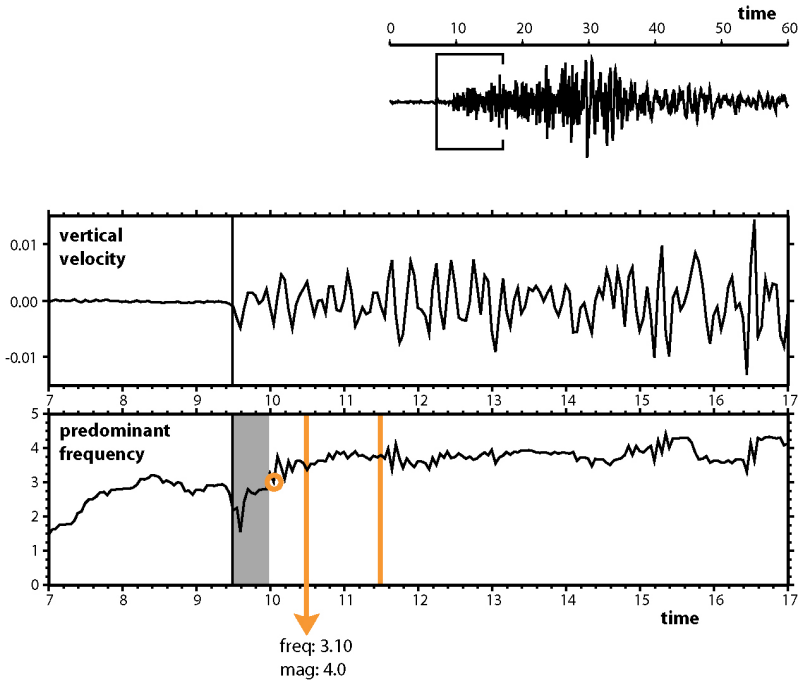

Fig. 3. Example magnitude estimation using the single station PDR 50 km from the epicenter of the January 29, 2002, magnitude 3.9, Simi Valley earthquake. The top trace shows the full vertical velocity waveform of which a 10 sec window is shown on the middle trace with the trigger time indicated by a vertical line. The bottom trace is the predominant frequency, f^p, calculated from the vertical velocity after low-passing the waveform at 10 Hz. Magnitude estimation proceeds as follows: (1) The first 0.5 sec of f^p is ignored as it contains transients. (2) The minimum f^p within 1 sec of the trigger, 3.10 Hz, is reported and converted to a magnitude of 4.0. (3) If a lower f^p is recorded within the 2nd second, it is reported and the magnitude estimate is updated to this larger magnitude (this does not occur in this example). Only 2 sec of data are used for small-magnitude events.

In a larger magnitude event both the low- and high-magnitude estimates are used as ElarmS updates the magnitude estimate. The example shown in Fig. 4 uses the vertical velocity trace from a station 82 km from the epicenter of the magnitude 7.1 Hector Mine earthquake. Initially the event is treated as a small-magnitude event: within the 1st second the minimum f^p observation is 2.82 Hz, corresponding to a magnitude of 4.2; in the 2nd second f^p drops to 1.78 Hz, providing a magnitude estimate of 5.5. A magnitude greater than 4.5 classifies the earthquake as a large-magnitude event causing the system to switch to using m_h. The minimum f^p (having low-passed the data at 3 Hz, Fig. 4) after 2, 3 and 4 sec is 0.99, 0.80 and 0.76 Hz corresponding to magnitude estimates of 5.9, 6.6 and 6.7 respectively. The final error in the magnitude estimate using this single station is 0.4.

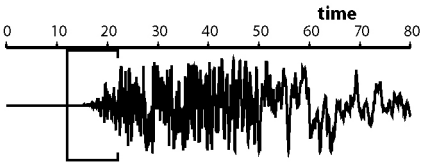

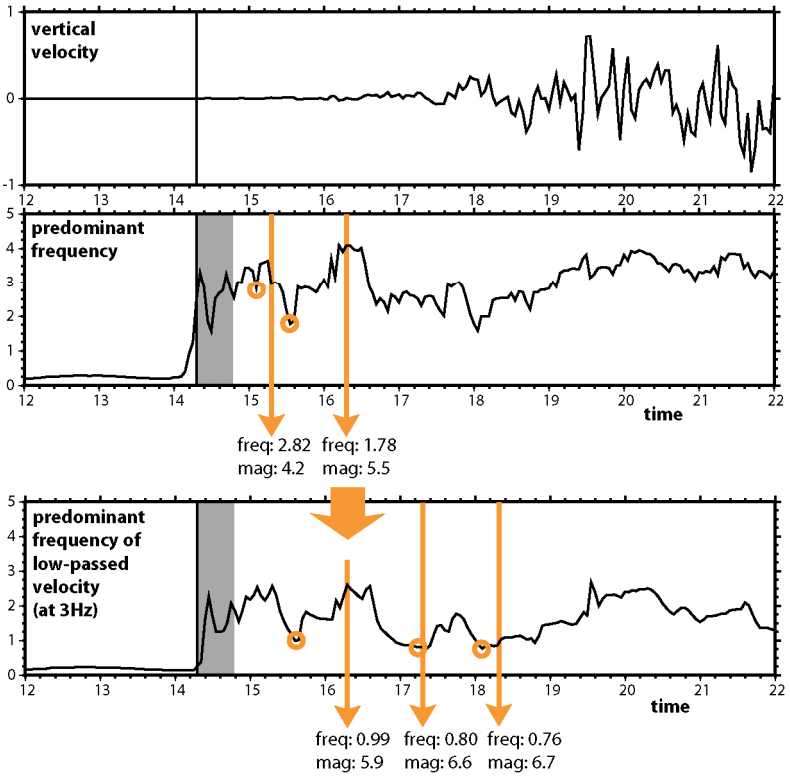

Fig. 4. Example magnitude estimation using the single station DAN 82 km from the epicenter of the October 16, 1999, magnitude 7.1, Hector Mine earthquake. The top three traces are the same as Fig. 3. Magnitude estimation proceeds as follows: (1) The first 0.5 sec of f^p is ignored as it contains transients. (2) The minimum f^p within 1 sec of the trigger, 2.82 Hz, is reported and converted to a magnitude of 4.2. (3) The minimum f^p within 2 sec of the trigger is lower, 1.78 Hz, corresponding to an updated magnitude of 5.5. This classifies the event as a large-magnitude earthquake. Therefore f^p is recalculated having low-passed the data at 3 Hz and will be monitored for 4 sec. The new minimum f^p within 2 sec is 0.99 Hz corresponding to a magnitude of 5.9 using the high-magnitude relation. (4) Within 3 sec the minimum f^p drops to 0.80 Hz and the magnitude is updated to 6.6. (5) Within 4 sec the minimum f^p drops again to 0.76 Hz providing a final magnitude estimate of 6.7.

The use of a dense seismic network in the earthquake source region provides for rapid event detection, location, and also multiple observations of $T^p_{\max}$ and corresponding magnitude estimates. The error in the event-magnitude estimate is rapidly reduced when multiple station-magnitude estimates are averaged. Table 1 shows the average absolute magnitude estimate for the dataset of 53 earthquakes in southern California. When only the closest station is used to estimate magnitude the average error is 0.7, when the closest 5 stations are averaged the error drops to 0.45, and with 10 stations the error is 0.35. For the purpose of early warning it is the speed with which accurate magnitude estimates are available that is important. To estimate how quickly magnitude estimates could be available in southern California a subset of 28 events is used. These are the events which occur within the dense portion of the seismic network (Fig. 1) and are also the events for which the most rapid hazard

estimates would be needed. Table 2 shows the proportion of events for which a magnitude estimate would be available and the average error with respect to the time of the S-wave arrival at the epicenter. The S-wave arrival at the epicenter is chosen as the reference time as it represents the earliest time of peak ground motion at the Earth's surface. It is also a conservative estimate as in larger magnitude events (the ones for which a warning would be needed) peak ground motion usually occurs several seconds after the S-wave arrival. In the case of southern California magnitude estimates could be available for 43% of events at the arrival time of the S-wave at the epicenter with an average error of 0.52. Magnitudes are available for 82% of events 2 sec later and the average error is 0.41.

Number of stations	Average magnitude error (magnitude units)
1	0.7
5	0.45
10	0.35

Table 1. The average absolute error in the event magnitude is reduced as more stations provide individual magnitude estimates that can be averaged.

Time after S-arrival at the epicenter (sec)	Proportion of events for which a magnitude estimate is available	Average magnitude error (magnitude units)
0	43%	0.52
2	82%	0.41
4	96%	0.29

Table 2. Case study showing the timing and accuracy of event magnitude estimates in southern California. The timing of magnitude estimates is reported relative to the S-wave arrival at the epicenter which represents the earliest possible timing of peak ground shaking at the surface.

3. Hazard predictor: attenuation relations

Given the location and magnitude of an earthquake the spatial distribution of predicted peak ground motion can be estimated using attenuation relations. Many different functional forms have been used for different types of earthquakes in different regions [e.g. *Campbell*, 1981; *Joyner and Boore*, 1981; *Fukushima and Irikura*, 1982; *Abrahamson and Silva*, 1997; *Boore et al.*, 1997; *Campbell*, 1997; *Sadigh et al.*, 1997; *Field*, 2000], however most are based on the functional form

$$A = A_0 r^n e^{-kr}$$

where A is the peak ground acceleration (PGA) at a distance r, and A_0, n and k are constants to be determined. This functional form has a term for geometric spreading, r^n, and one for intrinsic attenuation, e^{-kr}. Previously determined attenuation relations for southern California used only PGA observations for earthquakes with magnitudes greater than 5.5. Therefore, ElarmS uses its own attenuation relations that have been developed using observations from earthquakes ranging in magnitude from 3.0 to 7.3. It was found that the effect of intrinsic attenuation was not significant within 200 km of an event so k was set to zero to reduce the unknowns in the regression. n was determined as a function of magnitude by grouping PGA observations by magnitude and calculating the best fitting n. Having determined n, A_0 was calculated for each event and the best fitting linear relation between A_0 and magnitude was obtained. Fig. 5 shows how A_0 and n vary as a function magnitude.

ElarmS uses the attenuation relations in a two-stage process. One second after the first P-wave trigger the first estimate of magnitude is available. Given the magnitude, A_0 and n are determined from the relations shown in Fig. 5, and estimated PGA is calculated as a function of distance. As time progresses during the event sequence, the stations closest to the epicenter measure their PGA. Once this information is available from a few stations it is used to adjust the attenuation relation by keeping n fixed but allowing A_0 to change in order to best-fit the attenuation relation to PGA observations. Fig. 6 shows examples of the attenuation relations for magnitude 5.1, 6.1 and 7.1 earthquakes. Note the discrepancy between the observations and predictions of the *Field* [2000] attenuation relations. This discrepancy is a common problem when using attenuation relations determined from larger-magnitude

events only. The attenuation relations described here do not account for near-surface amplification effects, such as rock versus soil, which are responsible for much of the scatter in the acceleration observations shown in Fig. 6. Although site corrections are not currently part of ElarmS they can easily be included when known [e.g. *Wald et al.*, 1999a; *Wald et al.*, 1999b].

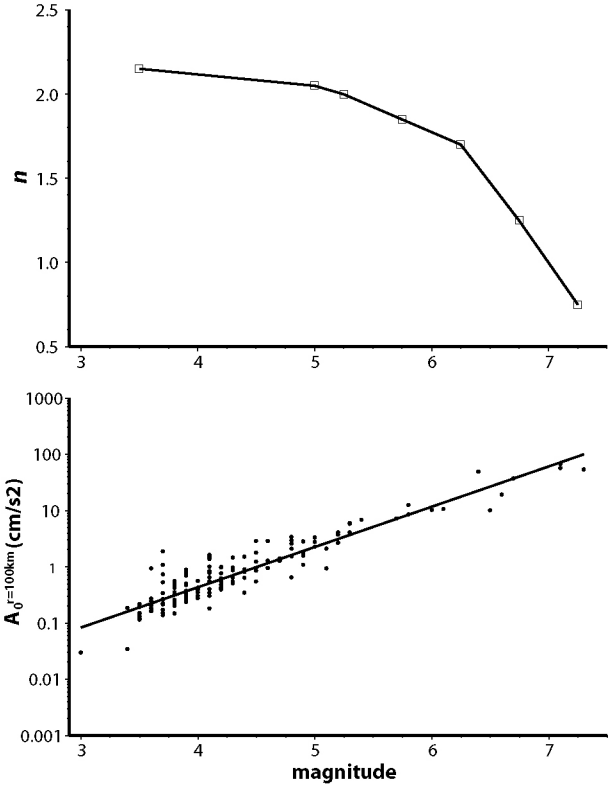

Fig. 5. Empirically determined values of n and A_0 as a function of earthquake magnitude. PGA observations were initially grouped by magnitude and n determined for each group by regression. Having determined n, the best fitting A_0 (defined as the amplitude at r=100 km) was calculated for each event. Linear regression provides A_0 as a function of magnitude.

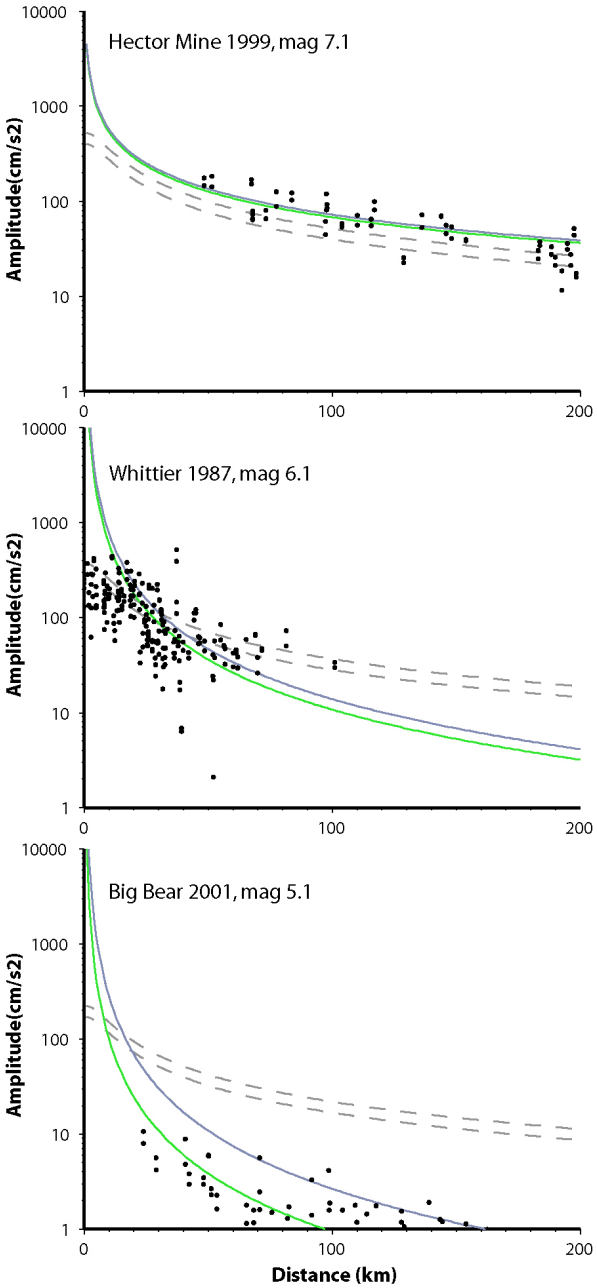

Fig. 6. Examples of attenuation relations (lines) and PGA observation (dots). (Top) The 1999, magnitude 7.1, Hector Mine earthquake. (Middle) The 1987, magnitude 6.1, Whittier earthquake. (Bottom) The 2001, magnitude 5.1, Big Bear earthquake. The grey lines show the ElarmS attenuation relations determined given just earthquake magnitude and the green lines are the result of adjusting the relation based on PGA observations. Dashed lines show the *Field* [2000] attenuation relations for rock and soil for comparison.

4. Notification system

The methodology presented above has the potential to provide zero to a few seconds of warning of forthcoming ground shaking at the epicenter. The warning time increases with distance from the epicenter: at 30 km approximately 10 sec of warning is possible; ~20 sec is available at 60 km. ElarmS is designed to provide a prediction of hazard as quickly as possible and then to update the prediction every second. The initial prediction is based on limited data and has the most uncertainty. As time proceeds, the initial stations provide more information and additional stations trigger, reducing the uncertainty in the hazard prediction along with the amount of warning time. The notification system should therefore allow users to decide on their tolerance for false alarms. For example, a school may decide to use the earliest warning possible because one or two false alarms per year can be considered as drills with little cost. However, an industrial user wishing to shut down a production line may decide that it would rather have less warning time but be more certain before a costly shut-down.

References

Abrahamson, N.A., and W.J. Silva, Empirical response spectral attenuation relations for shallow crustal earthquakes, *Seismological Research Letters*, *68* (1), 94-127, 1997.

Allen, R.M., and H. Kanamori, The Potential for Earthquake Early Warning in Southern California, *Science*, *300* (5620), 786-789, 2003.

Boore, D.M., W.B. Joyner, and T.E. Fumal, Equations for estimating horizontal response spectra and peak acceleration from western North American earthquakes; a summary of recent work, *Seismological Research Letters*, *68* (1), 128-153, 1997.

Campbell, K.W., Near-source attenuation of peak horizontal acceleration, *Bulletin of the Seismological Society of America*, *71* (6), 2039-2070, 1981.

Campbell, K.W., Empirical near-source attenuation relationships for horizontal and vertical components of peak ground acceleration, peak ground velocity, and pseudo-absolute acceleration response spectra, *Seismological Research Letters*, *68* (1), 154-179, 1997.

Field, E.H., A modified ground-motion attenuation relationship for southern California that accounts for detailed site classification and a basin-depth effect, *Bulletin of the Seismological Society of America*, *90* (6), S209-S221, 2000.

Fukushima, Y., and K. Irikura, Attenuation characteristics of peak ground motions in the 1995 Hyogo-ken, *J. Phys. Earth*, *45*, 135-146, 1982.

Hauksson, E., P. Small, K. Hafner, R. Busby, R. Clayton, J. Goltz, T. Heaton, K. Hutton, H. Kanamori, J. Polet, D. Given, L.M. Jones, and D. Wald, Southern California Seismic Network: Caltech/USGS Element of TriNet 1997-2001, *Seis. Res. Lett.*, *72* (6), 690-704, 2001.

Joyner, W.B., and D.M. Boore, Peak horizontal acceleration and velocity from strong-motion records including records from the 1979 Imperial Valley, California, earthquake, *Bulletin of the Seismological Society of America*, *71* (6), 2011-2038, 1981.

Kanamori, H., E. Hauksson, and T. Heaton, Real-time seismology and earthquake hazard mitigation, *Nature*, *390* (6659), 461-464, 1997.

Lockman, A., and R.M. Allen, Rapid magnitude determination for earthquakes in Japan and the Pacific Northwest, in preparation.

Nakamura, Y., On the Urgent Earthquake Detection and Alarm System (UrEDAS), *Proceedings of Ninth World Conference on Earthquake Engineering*, *VII*, 673-678, 1988.

Sadigh, K., C.Y. Chang, J.A. Egan, F. Makdisi, and R.R. Youngs, Attenuation relationships for shallow crustal earthquakes based on California strong motion data, *Seismological Research Letters*, *68* (1), 180-189, 1997.

Wald, D.J., V. Quitoriano, T.H. Heaton, and H. Kanamori, Relationships between peak ground acceleration, peak ground velocity, and Modified Mercalli Intensity in California, *Earthquake Spectra*, *15* (3), 557-564, 1999a.

Wald, D.J., V. Quitoriano, T.H. Heaton, H. Kanamori, C.W. Scrivner, and C.B. Worden, TriNet "ShakeMaps": Rapid generation of peak ground motion and intensity maps for earthquakes in southern California, *Earthquake Spectra*, *15* (3), 537-555, 1999b.